

# Subharmonic resonances in higher-order collision-enhanced wave mixing in a sodium-seeded flame

Rick Trebino and Larry A. Rahn

Combustion Research Facility, Sandia National Laboratories, Livermore, California 94550

Received June 22, 1987; accepted August 18, 1987

Using four-, six-, and eight-wave-mixing geometries, we observe subharmonic resonances in collision-enhanced spectra in a sodium-seeded hydrogen-air flame. Appearing at high intensity, these resonances occur at  $\pm 1/2$ ,  $\pm 1/3$ ,  $\pm 1/4$ , and  $\pm 1/5$  times the frequency of the ground-state hyperfine splitting  $\omega_{\text{hfs}}$ . We argue that these resonances result from higher-order processes, specifically  $\chi^{(n)}$ , where  $n \geq 5$ . In particular, to describe the resonances at  $\pm \omega_{\text{hfs}}/5$ , at least  $\chi^{(13)}$  is required. These high-order collision-enhanced effects are true perturbative nonlinearities and not sequential four-wave mixing processes.

Collisions can dephase quantum-mechanical amplitudes that ordinarily interfere destructively, thus generating otherwise forbidden resonances in nonlinear-optical processes.<sup>1</sup> Examples of such effects include collision-induced population gratings, coherences between unpopulated excited states, and collision-enhanced coherences between equally populated ground electronic states, all of which have been predicted and observed in four-wave mixing (4WM) experiments in atomic gases.<sup>1-4</sup> In this Letter we report the observation of collision-enhanced ground-state (Zeeman and hyperfine) resonances in a sodium-seeded hydrogen-air flame using high-resolution pulsed lasers. In non-degenerate 4WM experiments in this flame, we find that, at high intensities, additional spectral lines appear at the frequency differences  $\pm \omega_{\text{hfs}}/2$ , where  $\omega_{\text{hfs}}$  is the ground-state hyperfine splitting,  $0.059 \text{ cm}^{-1}$ . These subharmonic resonances appear to be due to higher-order wave-mixing processes. To verify this, we have performed additional experiments using  $N$ -wave-mixing (NWM) beam geometries, where  $N = 6$  and  $8$  (see Fig. 1a), that eliminate lower-order effects but that permit higher-order ( $N + 2$ ,  $N + 4$ , ...) effects. These experiments reveal subharmonics at  $\pm 1/2$ ,  $\pm 1/3$ ,  $\pm 1/4$ , and  $\pm 1/5$  of the hyperfine splitting, the last of which requires a nonlinear susceptibility of order at least as high as  $\chi^{(13)}$  for its explanation. While higher-order wave mixing is not new,<sup>5</sup> we believe that this is the first observation of *collision-enhanced* higher-order wave mixing.

A theory of collision-enhanced higher-order wave mixing was recently presented by Agarwal and Nayak,<sup>6</sup> who used a continued-fraction approach for a two-level system. This work predicted fractional resonances at the subharmonics of the Rabi frequency and has recently been extended to a three-level system<sup>7</sup> to predict subharmonic resonances between the two ground electronic states. Standard diagrammatic perturbation theory also predicts subharmonics in higher-order wave-mixing processes (see Fig. 1b), and we have used a diagrammatic perturbation-theory approach<sup>8</sup> to derive theoretical expressions for collision-enhanced 6WM that predicts subharmonic resonances.

In our experiments, two separately pulse-amplified, single-mode, cw dye lasers provide the  $\sim 590$ -nm light necessary to nearly excite the  $D_1$  line of sodium. Pulse amplification involves two separate three-stage, single-axial-mode Nd:YAG-pumped dye cells. The resulting 2-mJ, 20-nsec temporally Gaussian pulses have linewidths of  $< 60$  MHz. We split one of these beams into two pulses of approximately equal energy, and we label the two pulses by the frequencies and  $k$  vectors  $(\omega_1, \mathbf{k}_1)$  and  $(\omega_1, \mathbf{k}_1')$ , respectively. The frequency of the other beam, labeled by  $(\omega_2, \mathbf{k}_2)$ , is tunable. All three beams propagate, unfocused, into an approximately stoichiometric hydrogen-air flame seeded with sodium. We use a nonplanar 4WM geometry, in which the four beams of the interaction (three input beams plus the signal beam) appear as the corners of a square if observed end-on. In this configuration, both beams at frequency  $\omega_1$  are polarized vertically, while the beam at frequency  $\omega_2$  is polarized horizontally. The 6WM and 8WM geometries are planar, having the  $k$ -vector conservation equations  $\mathbf{k}_{\text{sig}} = 2(\mathbf{k}_1 - \mathbf{k}_2) + \mathbf{k}_1'$  and  $\mathbf{k}_{\text{sig}} = 3(\mathbf{k}_1 - \mathbf{k}_2) + \mathbf{k}_1'$ , respectively (see Fig. 1a). In both of these geometries, the beam polarizations are the same as in the 4WM arrangement. All geometries involve angles of  $\sim 3^\circ$  between  $\mathbf{k}_1$  and  $\mathbf{k}_2$ . Each beam's wavelength is about  $2 \text{ cm}^{-1}$  less than the  $D_1$  resonance frequency. Beam diameters at the flame are 5 mm, and the interaction length is limited by the flame thickness, about 2 mm. For 4WM experiments, the sodium concentration in the flame is of the order of 20 parts in  $10^6$  (ppm), while for 6WM and 8WM phase-matching experiments this value is 200 ppm ( $\sim 10^{15} \text{ cm}^{-3}$ ). We detect the wave-mixing signal energy with a photomultiplier tube and use a microcomputer for data acquisition and storage. The signal energy is normalized by an appropriate product of input laser energies on a shot-by-shot basis and then averaged for as many as 40 laser pulses for each data point. All spectra are necessarily collision enhanced because population densities of all ground electronic sublevels are equal.

Using the 4WM geometry and working at relatively low intensity ( $300 \text{ W/cm}^2$  per beam at the flame), we obtain the collision-enhanced 4WM spectrum shown

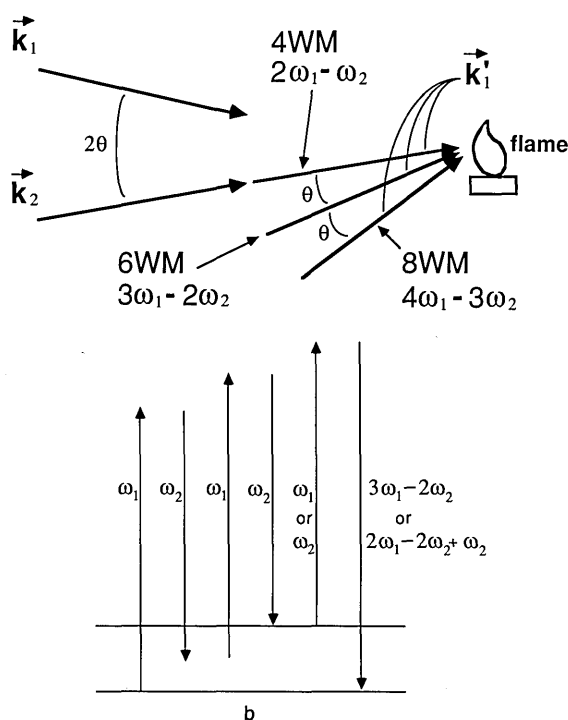


Fig. 1. a, 6WM and 8WM beam geometries using small-angle planar phase matching. A planar 4WM geometry is also shown for reference. These higher-order geometries exclude lower-order wave-mixing signals. b, Energy-level diagram for 6WM showing a four-photon  $[2(\omega_1 - \omega_2)]$  subharmonic resonance. The  $3\omega_1 - 2\omega_2$  process requires a 6WM geometry, while the  $2\omega_1 - 2\omega_2 + \omega_2$  process is phase matched in 4WM geometries.

in Fig. 2a, which shows the Zeeman resonance (at  $\delta \equiv \omega_1 - \omega_2 = 0$ ) and the hyperfine resonances (at  $\delta = \pm 0.06 \text{ cm}^{-1}$ ). This spectrum agrees quite well with the theoretical and experimental spectra of Rothberg and Bloembergen<sup>3</sup> for sodium in a heat-pipe oven. In Fig. 2b, the intensity is higher ( $20 \text{ kW/cm}^2$  per beam), and we see some saturation broadening of the 4WM spectrum. In addition, however, new spectral features are present at frequencies of about one half of the hyperfine resonance frequencies. There does not appear to be a 4WM explanation for these subharmonic resonances. Instead, we believe that the subharmonic resonances are due to collision-enhanced higher-order wave mixing.

To see that such an explanation is possible, we observe that, in general, a phase-matched NWM geometry is automatically phase matched for higher-order processes. Such a higher-order process can be constructed by adding and subtracting an input frequency from the signal-frequency expression and adding and subtracting the corresponding  $k$  vector from the signal  $k$ -vector expression. This creates a phase-matched  $(N + 2)$  WM process. Arbitrarily high-order processes can be obtained by adding and subtracting additional input frequencies and  $k$  vectors. For example, in the  $2\omega_1 - \omega_2$  4WM geometry, the 6WM process  $[2(\omega_1 - \omega_2)] + \omega_2$  and 8WM process  $[2(\omega_1 - \omega_2)] + \omega_2 - \omega_1 + \omega_1$  can occur, both having resonances at  $2(\omega_1 - \omega_2) = \pm \omega_{\text{hfs}}$ , i.e.,  $\omega_1 - \omega_2 = \pm \omega_{\text{hfs}}/2$ . Of course, even higher-order processes, having subharmonic res-

onances at  $\pm \omega_{\text{hfs}}/m$ , where  $m = 3, 4, \dots$ , are also possible. Specifically, the 10WM and 12WM processes,  $[3(\omega_1 - \omega_2)] + \omega_2 - \omega_1 + \omega_2$  and  $[(3(\omega_1 - \omega_2)] + 2(\omega_2 - \omega_1) + \omega_1$ , exhibit  $\pm \omega_{\text{hfs}}/3$  subharmonics. 14WM and 16WM processes exhibit  $\pm \omega_{\text{hfs}}/4$  subharmonics, etc.

Testing this hypothesis by using higher intensities, where higher-order wave mixing might be expected to increase further in strength relative to 4WM, fails, however, because the broadening increases also, smearing out the entire spectrum. Instead, we use a 6WM geometry, which eliminates—all 4WM contributions to the spectrum. Raj *et al.* have used a similar method in induced-grating experiments.<sup>9</sup> It is not difficult to find such a geometry, and the geometry that we chose is shown in Fig. 1. It is phase matched for processes of the form  $3\omega_1 - 2\omega_2$ , but it has difference-frequency resonances similar to those of the 6WM process  $[2(\omega_1 - \omega_2)] + \omega_2$  and the 8WM process  $[2(\omega_1 - \omega_2)] + \omega_2 - \omega_1 + \omega_1$ . Both of these last-named processes are automatically phase matched in  $2\omega_1 - \omega_2$  4WM experiments. On the other hand, this 6WM geometry is not phase matched for  $2\omega_1 - \omega_2$  4WM processes; thus it allows us to observe higher-order wave-mixing effects that appear in 4WM spectra, unobscured by the generally stronger 4WM effects.

Figure 3a shows a typical experimental 6WM geometry ( $3\omega_1 - 2\omega_2$ ) spectrum, acquired using  $7 \text{ kW/cm}^2$  in each of the three input beams. The central component, a Zeeman resonance at  $\delta = 0$ , is artificially attenuated by a factor of 50 by using neutral-density filters to avoid saturating the detection electronics. The four-photon-resonant subharmonic resonances are now quite clearly evident at  $\delta = \pm \omega_{\text{hfs}}/2 = \pm 0.03 \text{ cm}^{-1}$ . The two-photon-resonant hyperfine components are

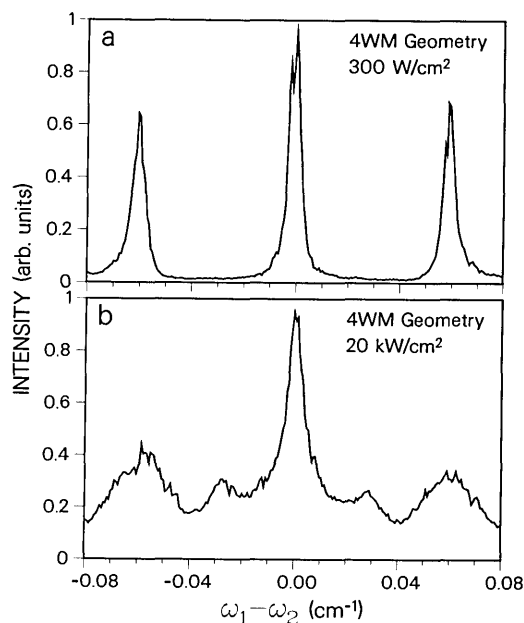


Fig. 2. a, 4WM spectrum of collision-enhanced Zeeman ( $\omega_1 - \omega_2 = 0$ ) and hyperfine ( $\omega_1 - \omega_2 = \pm \omega_{\text{hfs}} = \pm 0.06 \text{ cm}^{-1}$ ) resonances in sodium in a flame at low laser intensity. b, Same as a, except that much higher intensities illuminate the flame ( $20 \text{ kW/cm}^2$  peak per beam). Observe the additional subharmonic spectral components at  $\pm 0.03 \text{ cm}^{-1}$ .

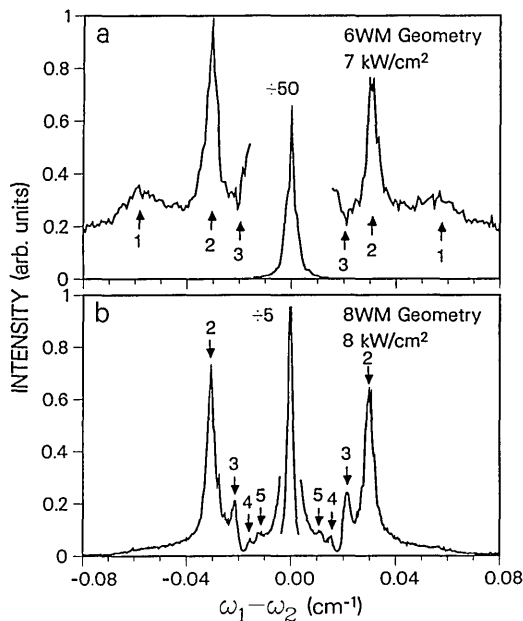


Fig. 3. a, Spectrum of collision-enhanced resonances in sodium in a flame obtained using a 6WM geometry ( $3\omega_1 - 2\omega_2$ , in lowest order). The phase-matching geometry shown in Fig. 1 limits the signal to six- and higher-order wave-mixing while retaining the same difference-frequency resonances that occur in 4WM geometries. Note the strong Zeeman resonance at zero frequency difference, the sharp four-photon subharmonic resonances at  $\pm 0.03 \text{ cm}^{-1}$  (labeled 2), and the weak two-photon hyperfine resonances at  $\pm 0.06 \text{ cm}^{-1}$  (labeled 1). Also observe the small dips at  $\pm 0.02 \text{ cm}^{-1}$  (labeled 3), which are probably due to six-photon resonances at  $\pm\omega_{\text{hfs}}/3$ . The small constant background is due to scattered light and is not a nonlinear-optical effect. b, Spectrum obtained using an 8WM geometry ( $4\omega_1 - 3\omega_2$ ). Observe the subharmonics at  $\pm 1/2$ ,  $\pm 1/3$ ,  $\pm 1/4$ , and  $\pm 1/5$  of the hyperfine splitting (labeled 2, 3, 4, and 5, respectively). The subharmonics at  $\pm\omega_{\text{hfs}}/5$  are due to at least 14WM.

also present, but weak, at  $\delta = \pm\omega_{\text{hfs}} = \pm 0.06 \text{ cm}^{-1}$ . In addition, careful observation at  $\delta = \pm\omega_{\text{hfs}}/3$  reveals dips in the wings of the Zeeman resonance line, indicating the presence of 8WM or higher-order processes.

We can rule out as a cause of this spectrum sequential 4WM processes, that is, 4WM with the signal beam acting as the input beam to another 4WM process, because at least one of the required 4WM processes is not phase matched. In addition, sequential processes do not yield subharmonics.

The use of an 8WM phase-matching geometry reveals additional subharmonics. Figure 3b shows a typical spectrum. Observe again the strong central Zeeman component. Note that the two-photon hyperfine resonance at  $\delta = \pm\omega_{\text{hfs}}$  is now extremely weak, while the  $\delta = \pm\omega_{\text{hfs}}/2$  subharmonics remain strong. The  $\delta = \pm\omega_{\text{hfs}}/3 = \pm 0.02 \text{ cm}^{-1}$  subharmonics now appear dispersive in shape, and new subharmonics now appear at  $\delta = \pm\omega_{\text{hfs}}/4 = \pm 0.015 \text{ cm}^{-1}$  and  $\delta = \pm\omega_{\text{hfs}}/5 =$

$\pm 0.012 \text{ cm}^{-1}$ . While 8WM processes can accommodate  $\pm\omega_{\text{hfs}}/2$  and  $\pm\omega_{\text{hfs}}/3$  subharmonics, at least 10WM is required for the  $\pm\omega_{\text{hfs}}/4$  subharmonic, and 14WM is the minimum-wave process that can yield  $\pm\omega_{\text{hfs}}/5$  subharmonics in our 8WM geometry.

At present, we have determined only the minimum order of wave mixing required to yield a given subharmonic. Selection rules forbid various  $N$ -wave processes, so that even higher-order wave-mixing processes must be invoked to explain some subharmonics. For example, the  $\pm\omega_{\text{hfs}}/2$  subharmonics in the 4WM geometry cannot result from 6WM processes because sample isotropy requires the 6WM probe and signal beams to have the same polarization, which carries the selection rule,  $\Delta F = 0$ . 8WM processes, on the other hand, are not forbidden and can yield this resonance. Selection rules for 4WM processes have been worked out by Rothberg and Bloembergen,<sup>3</sup> and we are at present calculating selection rules for higher-order hyperfine and Zeeman resonances. Experiments in a magnetic field, currently under way, should confirm the selection rules involved, for both hyperfine and Zeeman subharmonics. We are, however, at the limit of applicability of the perturbative expansion for  $\chi$ , and it will be of interest to compare these spectra with predictions from high-intensity theories, such as that of Agarwal.<sup>7</sup>

The authors would like to acknowledge the useful advice of G. S. Agarwal. This work was supported by the U.S. Department of Energy, Office of Basic Energy Sciences, Chemical Sciences Division.

## References

1. N. Bloembergen, in *Laser Spectroscopy IV*, H. Walther and K. W. Rothe, eds. (Springer-Verlag, Berlin, 1979), p. 340; Y. Prior, A. R. Bogdan, M. Dagenais, and N. Bloembergen, *Phys. Rev. Lett.* **46**, 111 (1981).
2. R. Trebino and L. A. Rahn, in *Advances in Laser Science II*, R. C. Powell, W. C. Stwalley, M. Lapp, G. A. Kenney-Wallace, and R. Gross, eds. AIP Conf. Proc. (to be published, 1987).
3. L. J. Rothberg and N. Bloembergen, *Phys. Rev. A* **30**, 820 (1984); L. J. Rothberg and N. Bloembergen, *Phys. Rev. A* **30**, 2327 (1984).
4. J. F. Lam, D. G. Steel, and R. A. McFarlane, *Phys. Rev. Lett.* **56**, 1679 (1986).
5. See, for example, V. F. Lukinykh, S. A. Myslivets, A. K. Popov, and V. V. Slabko, *Appl. Phys. B* **34**, 171 (1984); A. V. Smith, *Opt. Lett.* **10**, 341 (1985); P.-L. Zhang and A. L. Schawlow, *Can. J. Phys.* **62**, 1187 (1984).
6. G. S. Agarwal and N. Nayak, *Phys. Rev. A* **33**, 391 (1986).
7. G. S. Agarwal, University of Hyderabad, Central University P.O., Hyderabad-500134, India (personal communication).
8. R. Trebino and L. A. Rahn, "Higher-order collision-induced effects: a new diagrammatic approach," submitted to *Phys. Rev. A*.
9. R. K. Raj, Q. F. Gao, D. Bloch, and M. Ducloy, *Opt. Commun.* **51**, 117 (1984).